Electronic Supplementary Material (ESI) for New Journal of Chemistry.

Supplementary Information

for

Microscopic Chiral Pockets in Tris(chelated) Iridium(III) Complex as Sites for Dynamic Enantioselective Quenching

Kazuyoshi Takimoto,[a] Kenji Tamura,[b] Yutaka Watanabe,[a] Akihiko Yamagishi[c] and Hisako Sato[a]*

[a]Department of Chemistry, Graduate School of Science and Engineering, Ehime University, Matsuyama 790-8577, Japan

[b]National Institute for Materials Science, Tsukuba, Ibaraki 305-0044, Japan

[c]Department of Medicine, Toho University, Tokyo 274-8510, Japan

Contents

S9. Stereoselective adsorption of $[Ru(acac)_3]$ by an ion-exchange adduct of chiral $[Ir(bzq)_2(phen)]^+$ and synthetic hectorite

S10. Comparison of the stereochemical effects on saturated adsorption between $[Ir(bzq)_2(phen)]^+$ and $[Ru(phen)_3]^{2+}$

S1. CD spectra of the enantiomers of $[Ir(bzq)_2(phen)]^+$

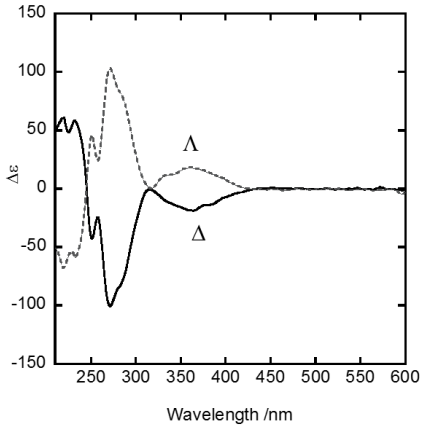

Figure S1. The CD spectra of the enantiomers of $[Ir(bzq)_2(phen)](ClO_4)$ dissolved in methanol. Solid and dotted curves are for the Δ- and Λ-isomers, respectively.

S2. Adsorption behavior of $[Ir(bzq)_2(phen)]^+$ by clay minerals

(1) Adsorption amounts versus the added amounts of clay minerals

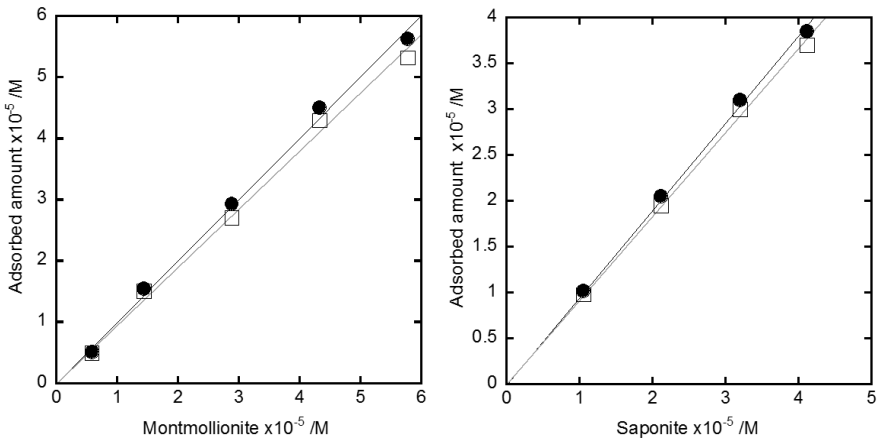

Figure S2. Adsorption amounts of racemic and enantiomeric complexes, when an exfoliated clay mineral was added to a 3:1 (v/v) water/methanol solution containing 1.0×10^{-4} M of $[Ir(bzq)_2(phen)](ClO_4)$: (left) sodium montmorillonite (MONT) and (right) synthetic saponite (SAP). The filled and open circles are for the racemic mixture and pure enantiomer, respectively.

(2) Equilibrium constants of adsorption by clay minerals

The equilibrium constant of adsorption was determined in the following procedure. An ion-exchange adduct of racemic $[Ir(bzq)_2(phen)]^+$ and montmorillonite or synthetic saponite (denoted as Ir(III)/MONT or Ir(III)/SAP, respectively) was dispersed in a 3:1 (v/v) water/methanol. After 6 hours, the dispersion was centrifuged. The concentration of dissociated $[Ir(bzq)_2(phen)]^+$ ions (or Ir(III)) was determined from the UV-vis spectrum of the filtrate. The equilibrium constant of adsorption (K_b) was calculated according to the equation below:

$$K_b = [\text{adsorbed Ir(III)}]/\ \{[\text{dissociated Ir(III)}]\ [\text{empty sites in a clay mineral}]\}$$

The results are shown in the following table.

Table S1. Equilibrium constant of adsorption

clay mineral	[dissociated Ir(III)]/M	[adsorbed Ir(III)]/M	[empty site in a clay mineral]/M	K_b/M^{-1}
MONT	1.4×10^{-6}	4.22×10^{-5}	1.4×10^{-6}	2.2×10^{7}
SAP	2.4×10^{-6}	3.22×10^{-5}	5.16×10^{-5}	2.6×10^{5}

(3) Improvement of optical purity of partially resolved $[Ir(bzq)_2(phen)]^+$ on adding sodium montmorillonite

The stereochemical effects on adsorption were studied in the following way. Sodium montmorillonite (MONT) was added to a 3:1 (v/v) water/methanol solution containing partially resolved $[Ir(bzq)_2(phen)](ClO_4)$. After the dispersion was centrifuged, the UV-vis and CD spectra of the filtrate were measured to determine the optical purity of the filtrate. The results were given in the table below. According to them, $[Ir(bzq)_2(phen)]^+$ showed the tendency that it preferred to be adsorbed as a racemic mixture rather than as an enantiomer.

Table S2. Improvement of optical purity of partially resolved $[Ir(bzq)_2(phen)]^+$ on adding MONT

	Before adding MONT	After adding MONT
Free Λ-isomer/M	0.97×10^{-5}	0.77×10^{-5}
Free racemic mixture /M	2.12×10^{-5}	1.10×10^{-5}
optical purity (e.e.)/%	31	41
added MONT/M		1.24×10^{-5}
adsorbed Λ-isomer/M		0.97×10^{-5}
adsorbed racemic mixture /M		2.12×10^{-5}
tendency of racemic adsorption (α)*		1.53

*The tendency of racemic adsorption (α) was estimated according to the following equation:

α = {[adsorbed racemic mixture]/[free racemic mixture]}/{[adsorbed Λ-isomer]/[free Λ-isomer]}

S3. Quantum yield of the emission from $[Ir(bzq)_2(phen)]^+$ in various solvents

Table S3. The peak wavelength and quantum yield of the emission from racemic $[Ir(bzq)_2(phen)](ClO_4)$ in various solvents*

Solvent	Concentration /M	peak wavelength /nm	quantum yield (Q.Y.)
CH_2Cl_2	4.4×10^{-5}	571	0.26
$CHCl_3$	3.9×10^{-5}	573	0.20
CH_3OH	3.6×10^{-5}	579	0.09
C_2H_5OH	2.7×10^{-5}	576	0.12
CH_3CN	4.4×10^{-5}	581	0.07
$(CH_3)_2CO$	3.9×10^{-5}	580	0.08

*) Quantum yield was calculated according to the following equation:

$$\Phi = \Phi_{st}(\frac{A_{st}}{A})(\frac{D}{D_{st}})(\frac{n^2}{n_{st}^2})$$

where Φ is quantum yield (Q.Y.) for an iridium(III) complex, A absorbance at 430 nm, D an irradiated area, n refractive index. The subscript st means the standard value for $[Ru(bpy)_3]^{2+}$ (Φ_{st} = 0.028). The wavelength of excitation (λ_{ex}) was 430 nm (ref. K. Nakamaru, *Bull. Chem. Soc. Jpn.,* 1982, **55**, 2697-2705).

S4. Emission spectra of $[Ir(bzq)_2(phen)]^+$ in clay suspensions

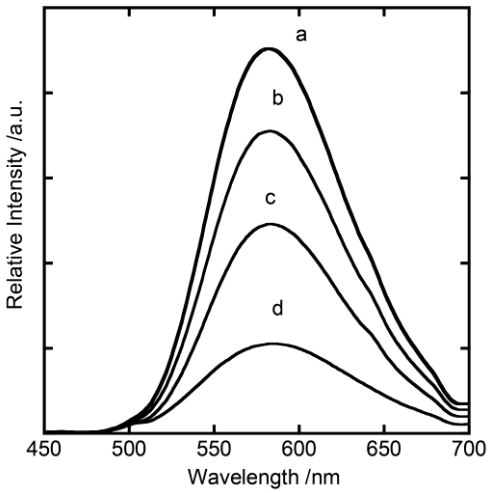

Figure S3 (a). The effects of synthetic saponite (SAP) on the emission spectra of racemic $[Ir(bzq)_2(phen)](ClO_4)$. A medium was 3:1 (v/v) water/methanol containing 4.70×10^{-6} M of $[Ir(bzq)_2(phen)](ClO_4)$ and various concentrations of SAP. The concentration of SAP was (a) 5.0×10^{-5}, (b) 2.5×10^{-5}, (c) 5.0×10^{-6}, (d) 0 eqL^{-1}, respectively. Excitation wavelength was 430 nm.

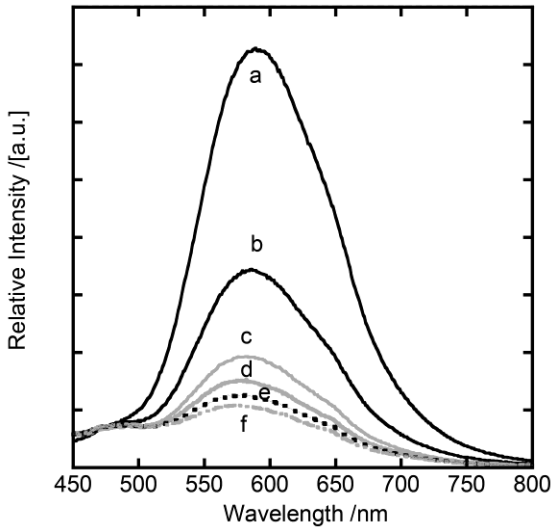

Figure S3 (b). The effects of sodium montmorillonite (MONT) on the emission spectra of racemic $[Ir(bzq)_2(phen)](ClO_4)$. A medium was 3:1 (v/v) water/methanol containing 7.00×10^{-6} M of $[Ir(bzq)_2(phen)](ClO_4)$ and various concentrations of MONT. The concentration of MONT was (a) 0, (b) 0.44×10^{-5}, (c) 1.10×10^{-5}, (d) 2.20×10^{-5}, (e) 4.40×10^{-5} and (f) 11.0×10^{-5} eqL^{-1}, respectively. Excitation wavelength was 430 nm.

S5. Stereochemical effects of the emission from $[Ir(bzq)_2(phen)]^+$ adsorbed by synthetic saponite

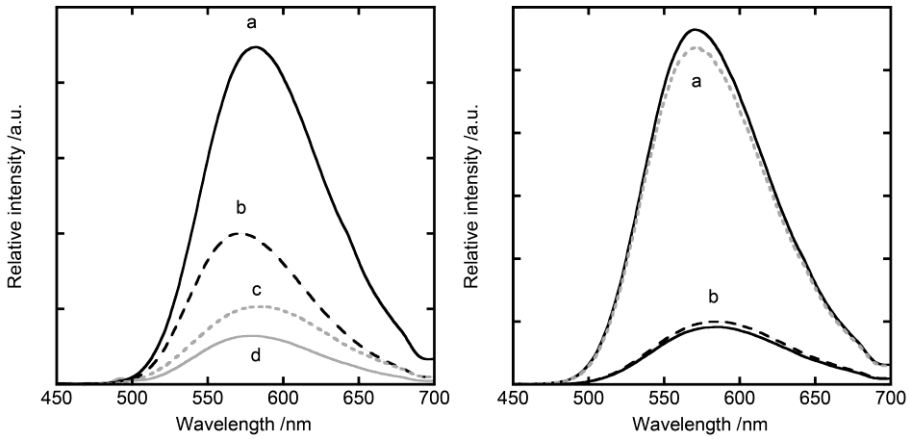

Figure S4 (left). The emission spectra of racemic $[Ir(bzq)_2(phen)]^+$ adsorbed by synthetic saponite (SAP). A medium was (a) 3:1 (v/v) water/methanol containing 5.00×10^{-6} M of $[Ir(bzq)_2(phen)](ClO_4)$ and 7.0×10^{-5} eqL^{-1} of SAP, (b) dichloromethane, (c) 3:1 (v/v) water/methanol and (d) methanol, respectively. Excitation wavelength was 430 nm

Figure S4 (right). The emission spectra of Δ- (solid) and Λ- (dotted) $[Ir(bzq)_2(phen)]^+$ adsorbed by synthetic saponite (SAP). A medium was (a) 3:1 (v/v) water/methanol containing 5.00×10^{-6} M of $[Ir(bzq)_2(phen)](ClO_4)$ and 7.0×10^{-5} eqL^{-1} of SAP and (b) 3:1 (v/v) water/methanol, respectively. Excitation wavelength was 430 nm.

S6. Enhancement of the luminescent quantum yield of $[Ir(bzq)_2(phen)]^+$ adsorbed by synthetic saponite

The quantum yield and the decay life-time were compared for racemic $[Ir(bzq)_2(phen)]^+$ between 1:1 (v/v) water/methanol and 1:1 (v/v) water/methanol/SAP. The obtained quantum yield (Q. Y), k_r and k_{nr} are shown in the table below:

Medium	Quantum yield (Q. Y.)(Φ)	Lifetime /μs (τ) at 570 nm	k_r /sec	k_{nr} /sec
1:1(v/v) water/methanol	0.21	0.16	1.30×10^6	4.88×10^6
1:1(v/v) water/methanol/SAP	0.39	0.37	1.05×10^6	1.65×10^6

In the above table, the concentration of $[Ir(bzq)_2(phen)](ClO_4)$ was 9.8×10^{-6} M at [SAP] = 1.0×10^{-4} eqL^{-1} . Quantum yield (Q.Y.) and lifetime were related to k_r and k_{nr} as below:

$$\Phi = \frac{k_r}{k_r + k_{nr}}$$

$$\tau = \frac{1}{k_r + k_{nr}}$$

where τ is lifetime at 570 nm, k_r the emissive rate constant and k_{nr} the non-radiative decay constant, respectively. On the basis of the above results, it was concluded that the enhancement of emission intensity for the clay-chelate hybrid was caused by the lowering of k_{nr} (or non-radiative decay rate). As stated in the text, it was due to the dehydration of an adsorbed chelate on a clay surface.

S7. Quenching effects of $[Ru(acac)_3]$ on the emission from $[Ir(bzq)_2(phen)]^+$ adsorbed by synthetic saponite

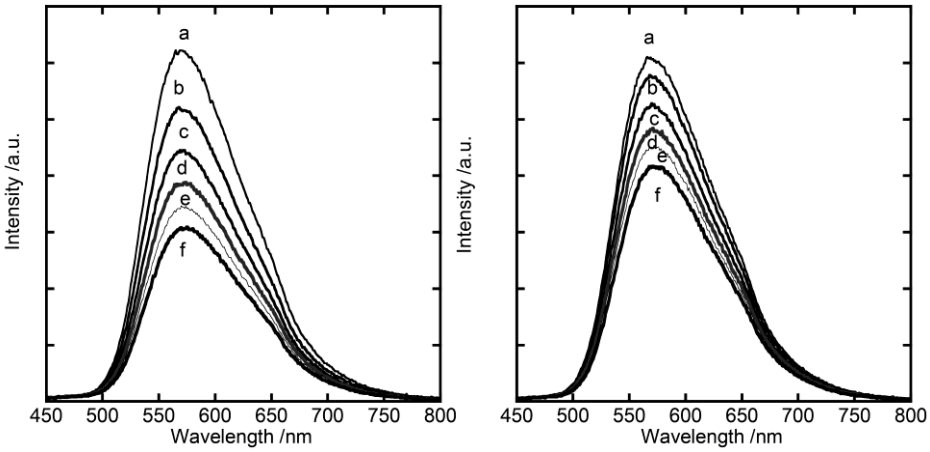

Figure S5. The effects of $[Ru(acac)_3]$ on the emission of $[Ir(bzq)_2(phen)]^+$ adsorbed by synthetic saponite (SAP). The emission spectra were measured in 3:1 (v/v) water/methanol containing $[Ir(bzq)_2(phen)]^+$ (4.2×10^{-6} M) and SAP (8.2×10^{-4} eqL^{-1}): (left) Λ-$[Ir(bzq)_2(phen)]$/Λ-$[Ru(acac)_3]$ and (right) Λ-$[Ir(bzq)_2(phen)]$/Δ-$[Ru(acac)_3]$. The added concentration of $[Ru(acac)_3]$ was (a) 0 M, (b) 1.2×10^{-5} M, (c) 2.4×10^{-5} M, (d) 3.6×10^{-5} M, (e) 4.8×10^{-5} M and (f) 6.0×10^{-5} M. Excitation wavelength was 430 nm.

S8. Stern-Volmer plots for the quenching of the emission from $[Ir(bzq)_2(phen)](ClO_4)$ by $[Ru(acac)_3]$ in methanol.

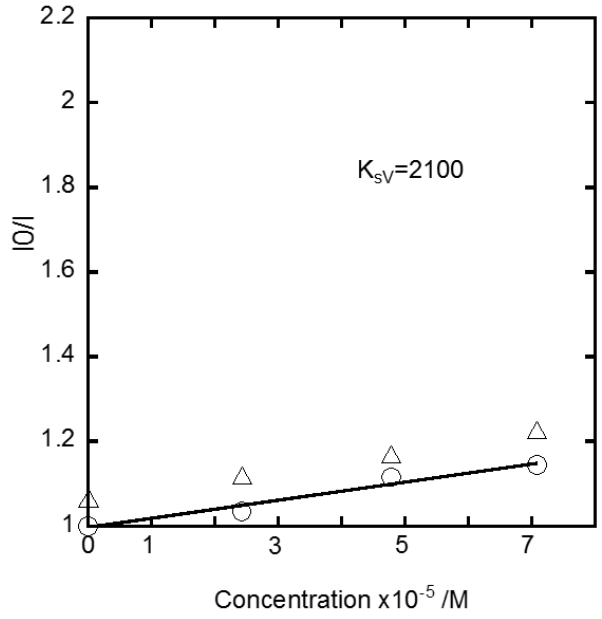

Figure S6. Stern-Volmer plots for the quenching effect by $[Ru(acac)_3]$ in methanol. The concentration of $[Ir(bzq)_2(phen)](ClO_4)$ was 4.2×10^{-6} M**:** (triangle) Δ-$[Ir(bzq)_2(phen)]^+$/Λ-$[Ru(acac)_3]$ and (circle) Δ-$[Ir(bzq)_2(phen)]^+$/ Δ-$[Ru(acac)_3]$. Excitation wavelength was 430 nm.

S9. Stereoselective adsorption of [Ru(acac)$_3$] by an ion-exchange adduct of chiral [Ir(bzq)$_2$(phen)]$^+$ and synthetic hectorite

Δ-[Ir(bzq)$_2$(phen)](ClO$_4$) (1.0×10^{-5} mole) was added to a 5 mL of methanol dispersion containing 50 mg of synthetic hectorite (Laporte Inc. Co.; denoted as HEC). The dispersion was centrifuged, leaving a precipitate of an ion-exchange adduct of Δ-[Ir(bzq)$_2$(phen)]$^+$/HEC. The adduct was dispersed in a 5 mL of methanol solution containing racemic 2.0×10^{-5} mole of [Ru(acac)$_3$]. After being stirred for 1 hour at room temperature, the dispersion was centrifuged. The filtrate (dented as *F*) was replaced with 5mL of pure methanol. The dispersion was stirred for 1 hour at room temperature. The filtrate was denoted as *P*. The CD spectra of *F* and *P* were measured and shown below. The results exhibited that *F* and *P* contained the small excesses of Λ- and Δ-enantiomers of [Ru(acac)$_3$], respectively. It implied that Δ-[Ru(acac)$_3$] was adsorbed by Δ-[Ir(bzq)$_2$(phen)]$^+$/HEC more strongly than Λ-[Ru(acac)$_3$].

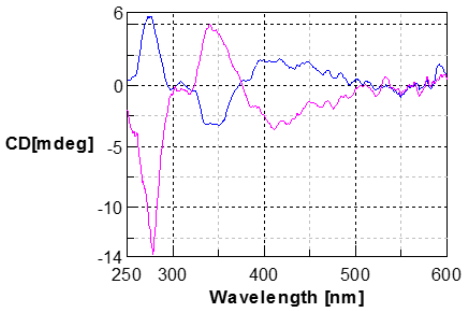

Figure S7. The CD spectra of *F* (pink) and *P* (blue). The results showed that *F* and *P* contained Λ-[Ru(acac)$_3$] and Δ-[Ru(acac)$_3$] as an excessive enantiomer, respectively.

S10. Comparison of the stereochemical effects of saturated adsorption between $[Ir(bzq)_2(phen)]^+$ and $[Ru(phen)_3]^{2+}$

The different behavior between $[Ir(bzq)_2(phen)]^+$ and $[Ru(phen)_3]^{2+}$ as to the stereochemical effects on the saturated adsorption amount is rationalized in terms of the balance of the electrostatic repulsion and van der Waals attraction as below:

1) In case of $[Ru(phen)_3]^{2+}$, the enantiomer is adsorbed within the CEC of a clay, while the racemic mixture is adsorbed to two times excess of CEC (ref. A. Yamagishi and H. Sato, *Clays and Clay Miner.*, 2012, **60**, 411).The enantiomeric chelate is adsorbed, leaving a vacant space on a surface ((A) in the scheme below), while the racemic chelate is adsorbed, covering fully a clay surface ((B) in the scheme below). The excess adsorption for the racemic case is realized due to the close packing of a racemic pair like a key-and-lock way. In other words, the van der Waals attraction surmounts the electrostatic repulsion between the adsorbed chelates. The enantiomeric chelate is unable to attain such close packing due to the steric hindrance between the ligands.

2) In case of $[Ir(bzq)_2(phen)]^+$, both the enantiomeric and racemic chelates are adsorbed within the CEC of a clay. They cover fully the surface of a clay surface ((C) and (D) in the scheme below, respectively). The enantiomeric chelate is able to attain such high density, since the electrostatic repulsion between the adsorbed chelates is low due to their monovalent charges.

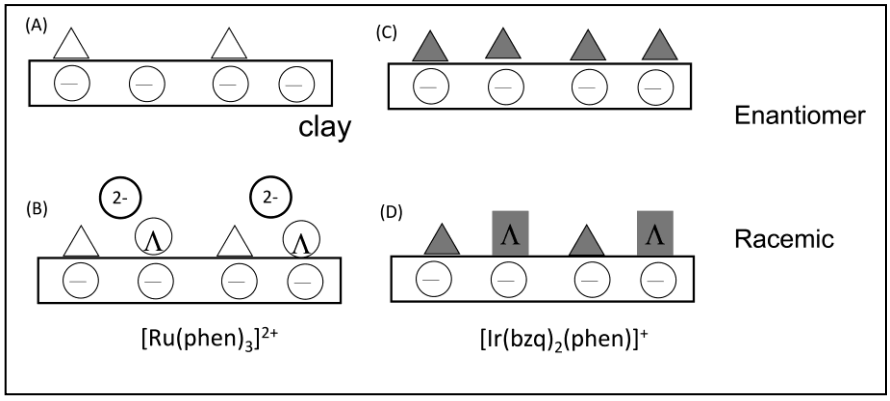

Scheme S1.

A. The enantiomeric adsorption of divalent $[Ru(phen)_3]^{2+}$ within the CEC of a clay layer.

B. The racemic adsorption of divalent $[Ru(phen_{)3}]^{2+}$ in excess over the CEC of a clay layer. External anions are co-adsorbed to compensate the positive charge.

C. The enantiomeric adsorption of monovalent $[Ir(bzq)_2(phen)^{]+}$ within the CEC of a clay.

D. The racemic adsorption of monovalent $[Ir(bzq)_2(phen)]^+$ within the CEC of a clay.